

Review

Integrating Small Animal Irradiators with Functional Imaging for Advanced Preclinical Radiotherapy Research

Mihaela Ghita ¹, Kathryn H. Brown ¹, Olivia J. Kelada ^{2,3}, Edward E. Graves ⁴ and Karl T. Butterworth ^{1,*} 

¹ Centre for Cancer Research and Cell Biology, Queen's University Belfast, Belfast BT9 7AE, Northern Ireland, UK; m.ghita@qub.ac.uk (M.G.); kbrown40@qub.ac.uk (K.H.B.)

² Molecular Imaging Program, National Cancer Institute, National Institutes of Health, Bethesda, MD 20892-1088, USA; olivia.kelada@nih.gov

³ In vivo Imaging, Discovery and Analytics, PerkinElmer Inc., Hopkinton, MA 01748, USA

⁴ Department of Radiation Oncology, Stanford University, Stanford, CA 94305-5152, USA; egraves@stanford.edu

* Correspondence: k.butterworth@qub.ac.uk; Tel.: +44-2890-972307

Received: 14 December 2018; Accepted: 29 January 2019; Published: 1 February 2019



Abstract: Translational research aims to provide direct support for advancing novel treatment approaches in oncology towards improving patient outcomes. Preclinical studies have a central role in this process and the ability to accurately model biological and physical aspects of the clinical scenario in radiation oncology is critical to translational success. The use of small animal irradiators with disease relevant mouse models and advanced in vivo imaging approaches offers unique possibilities to interrogate the radiotherapy response of tumors and normal tissues with high potential to translate to improvements in clinical outcomes. The present review highlights the current technology and applications of small animal irradiators, and explores how these can be combined with molecular and functional imaging in advanced preclinical radiotherapy research.

Keywords: preclinical radiotherapy; functional imaging; small animal irradiators; radiobiology; radiation oncology

1. Introduction

Since the introduction of the linear accelerator into the practice of radiation oncology during the 1950s, the discipline has undergone major technology changes that have significantly advanced all stages of the radiotherapy process from treatment planning to delivery and verification. These innovations have resulted in an unparalleled ability to delineate target volumes, conform radiation dose and irradiate under image guidance [1], which have translated to better tumor control and reduced toxicity in many cancer types. Despite these advances, it is unlikely that radiotherapy technology has reached its zenith, with many developments in molecular and functional imaging, treatment adaptation and particle therapy yet to be fully realized in the clinic [2].

In contrast, the impact of biologically driven strategies in radiation oncology has been less substantial. This is evidenced by the implementation of most advanced radiotherapy techniques on the basis of technology rather than a comprehensive understanding of radiobiological response, highlighting the need for advanced preclinical systems capable of modelling aspects of human disease under clinically relevant radiation exposure conditions. In addition, several radiotherapy clinical trials have reported null outcomes, an issue that was examined by the National Cancer Institute (NCI)

Radiation Research Program (RRP) at a workshop aiming to better understand these findings and to try to improve the success of future trials [3].

From radiotherapy trials reporting negative and null outcomes, an intriguing example is that of the phase 3 Radiotherapy Oncology Trial Group (RTOG) 0617 study. This aimed to compare standard-dose versus dose escalation with concurrent chemotherapy and the addition of cetuximab in patients with inoperable stage III non-small-cell lung cancer (NSCLC). The study failed to demonstrate overall survival benefit at the higher dose of 74 Gy, compared with the lower, standard dose of 60 Gy [4], and further reported 17 deaths in the high dose arms compared to 7 in the lower dose cohort. The causes of these unexpected findings have been explored with secondary analysis suggesting that deaths related to the effects of dose to the heart and lung are the most likely explanation of the findings, and these continue to be discussed [5].

Importantly, trials such as a RTOG 0617 need to be reverse translated using relevant preclinical models to gain *de novo* mechanistic insight into the clinical benefits and risks of dose escalation. Part of the recommendations proposed by the NCI RRP group have included the requirement for robust preclinical supporting data to guide subsequent clinical trials. In addition, Stone et al., surveyed data from 125 published reports which tested the interaction of 10 drug-radiation combinations and provided comprehensive recommendations for improved preclinical testing [6]. This has also been supported by further recommendations from Coleman et al., aiming at improve the predictive power of preclinical models in developing radiotherapy clinical trials [7]. Cumulatively, these reports clearly highlight the need for robust preclinical supporting data in translationally relevant disease models to justify radiotherapy clinical trials. In this context, it is essential that preclinical models in radiobiology research accurately reflect modern clinical practice, in terms of both biological model and physical radiation exposure conditions [8]. These approaches should also be further synergized with anatomical, functional and molecular imaging to optimize radiotherapy planning and response monitoring and maximize potential for translation. In this article, we review the technology of small animal irradiators and preclinical imaging techniques to identify key opportunities for translational research that may impact the future success rate of radiotherapy clinical trials.

2. Small Animal Radiotherapy: Rationale and Technology

Since the first report of the tissue sparing effects from fractionation in ram testes more than 100 years ago [9], small animal models have been widely applied in radiobiological studies predicated on the basis of genetic and physiological similarities with humans [10]. In particular, mouse models have contributed significantly to the advancement of biomedical research [11]. Recent genome editing technologies continue to allow a wide spectrum of gain- and loss-of-function mutations to be investigated along with evaluation of novel therapies in defined genomic backgrounds. In addition, the implantation of human tissue into NOD-scid- γ (NSG) mice with partially reconstituted immune systems can help to recapitulate aspects of the patient immune response during treatment through humanized mouse models [12]. Whilst no ideal mouse model exists to truly recapitulate the human setting, it is important that contemporary disease models are used with advanced irradiation techniques to closely mimic clinical scenarios and maximize the potential to deliver translationally relevant datasets [13].

Classic radiobiology experiments have been performed using broad fields from fixed sources and shielding to target the beam. Some of these experiments involved the irradiation of large volumes (usually whole body or whole thorax) which did not require precision image guidance, however, these procedures have high levels of uncertainty due to inaccurate beam targeting, as highlighted in Figure 1.

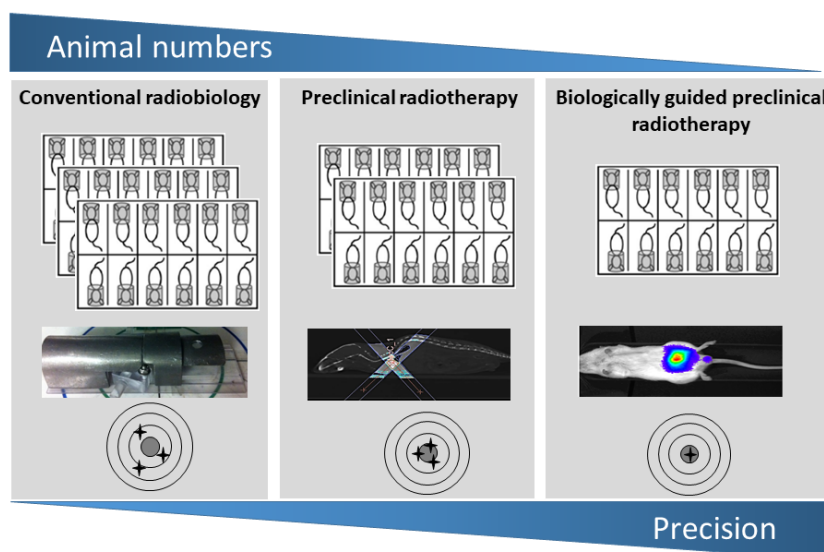


Figure 1. Schematic diagram demonstrating the evolution of conventional radiobiology to image-guided preclinical radiotherapy and molecular imaging. These changes are a major refinement of conventional techniques and have resulted in improved precision and accuracy. Overall, these advanced approaches have reduced study sizes in radiobiology studies required to obtain statistical power by reducing dose uncertainty, error and allowing longitudinal analysis.

Similar to clinical techniques, modern radiobiology studies aim to irradiate small target volumes with high levels of precision and accuracy. Devices capable of performing image-guided irradiation in small animals have been developed over the last 10 years by a number of investigators and vendors (Table 1). Two systems have been made commercially available: The Small Animal Radiotherapy Research Platform (SARRP) from Xstrahl Life Sciences developed at Johns Hopkins University [13] and the X-Rad SmART from Precision X-ray Inc., developed at Princess Margaret Hospital [14]. In addition, several other systems have been designed and implemented at a number of institutions across the world using approaches consisting of rotating or fixed gantries with cone beam computed tomography (CBCT) detectors or conversions of micro-CT devices. Details of these systems and their characteristics are summarized in Table 1.

Table 1. Summary of small animal radiotherapy systems and individual characteristics.

Research Platform	Vendor Research Institute	Beam Energy (KeV)	Dose Rate (Gy/Min)	Beam Collimation	Accuracy (mm)	Image Guidance	Treatment Planning System	Reference
Commercially available								
SARRP ¹	Xstrahl Life Sciences	5–225	1–4	Aperture MVC	0.2	CBCT BLT	Muriplan	[14,15]
X-RAD 225Cx SmART ²	Precision X-ray	5–225	0.01–4	Aperture	0.2	CBCT BLI	SmART-Plan	[16]
Non-commercial								
iSMAART	University of Miami, USA	45–225	2.5–4	Aperture	0.4	CBCT BLT FLT	In house	[17–19]
SAIGRT ³	Technical University of Dresden, Germany	10–225	1–4	Aperture MVC	0.1	CBCT	In house	[20]

Table 1. Cont.

Research Platform	Vendor Research Institute	Beam Energy (KeV)	Dose Rate (Gy/Min)	Beam Collimation	Accuracy (mm)	Image Guidance	Treatment Planning System	Reference
Non-commercial								
SACRTD ⁴	University of Arkansas, AR, USA	60–225	0.4–3	Aperture	0.2	CBCT	In house	[21]
Micro-CT based radiotherapy devices	Stanford University, USA	70–120	2	Aperture	<0.1	CBCT	In house	[22]
	Heidelberg University, Germany	10–160	4.5–6.4	Aperture	<1	CBCT	In house	[23]
	The University of Western Ontario, Canada	70–140	2	Jaw Collimation	0.1	CBCT	In house	[24]

¹ Small animal radiotherapy research platform (SARRP); ² Small animal radiotherapy (SmART); ³ Small animal image guided radiotherapy (SAIGRT); ⁴ Small animal conformal radiotherapy device (SACRTD).

To complement these platforms, dedicated treatment planning systems (TPS) analogous to those used clinically are required for accurate dose calculations. These have been developed using the superposition convolution algorithm [25], Monte Carlo simulations [15] or in-house dose engines [26]. Preclinical TPS aim to efficiently solve the challenges associated with tissue segmentation and dose calculation relating to photon scattering for very small fields and differences in the energy absorption of soft tissues for kilovoltage beams [27]. Although still at a relatively early stage, small animal irradiators are rapidly becoming the experimental standard in radiobiology. Previously unachievable experimental approaches are now being explored, including the irradiation of small target volumes (under 100 mm³) at depth under image guidance from computed tomography (CT), magnetic resonance imaging (MRI) and bioluminescence imaging (BLI).

The integration of small animal irradiators into radiobiology research either, simultaneously or sequentially combined with imaging methods such as CT, BLI, positron-emission tomography (PET) and MRI, have significantly improved the level of precision and accuracy with which target volumes can be irradiated. These strategies have directly impacted animal welfare within the framework of the UK National Centre for the Replacement, Refinement and Reduction of Animals in Research (NC3Rs). In particular, these improvements are a major refinement from conventional approaches as both precision and accuracy has been improved along with the ability to acquire longitudinal information from the same animals. Consequently, this has reduced the requirement for large study sizes which shown schematically in Figure 1 [28,29].

3. Preclinical Imaging: Principles and Technology

Imaging has focused on the visualization of anatomical regions of interest in the diagnosis and staging of disease, as well as monitoring response to therapy. Conventional anatomical imaging methods, such as X-ray, fluoroscopy and computed tomography (CT) continue to play a critical role in the delineation of macroscopic patient anatomy. However, advances in molecular biology have enabled imaging techniques to move beyond structural characterization of malignancy into the realm of molecular imaging [30]. This involves the visualization, characterization, and measurement of biological processes at the molecular and cellular levels, typically including two- or three-dimensional imaging using techniques such as PET, Single Photon Emission Computed Tomography (SPECT) and BLI [31]. Some of these techniques overlap as functional imaging modalities that are used to delineate and measure physiologic functions in organ systems, including techniques such as PET, functional MRI and ultrasound.

Many preclinical imaging techniques were originally developed as clinical imaging procedures but have since been reverse translated in the same way modern radiotherapy has been brought to the preclinical laboratory. A variety of imaging methods are now available to plan and monitor radiotherapy response in a manner analogous to that in the clinic as shown in Figure 2.

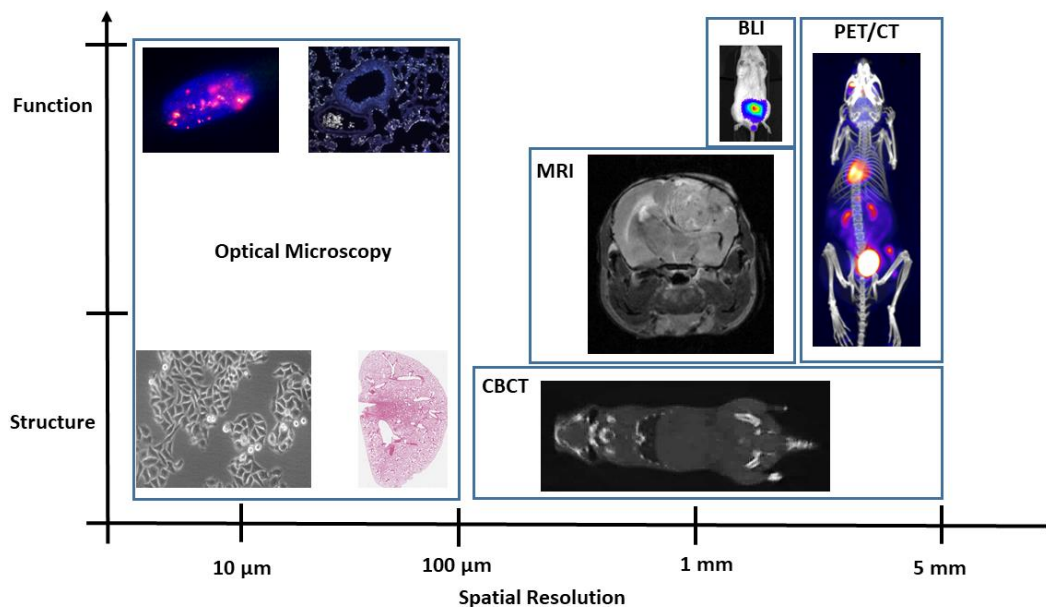


Figure 2. Schema of different preclinical imaging techniques showing increasing molecular specificity and spatial resolution for in vitro and in vivo studies. BLI, bioluminescence imaging; PET, positron-emission tomography; CT, computed tomography; MRI, magnetic resonance imaging.

X-ray computed tomography (CT) remains the primary imaging modality in preclinical and clinical radiotherapy treatment planning. In small animal CT scanners, X-rays are emitted as a beam from the tube, pass through the subject and are detected by a large-area solid-state radiation detector [28]. Whilst CT can provide material composition information useful for dose calculation, it has limited soft tissue contrast that can complicate identification of targets for treatment as well as volumes of radiosensitive tissues to be avoided.

A variety of molecular imaging technologies have been developed that generate image contrast based on functional aspects of tissue including perfusion, gene expression, oxygenation and metabolism, rather than anatomical structure [28,32–34]. The most prominent modality used for this purpose clinically is positron-emission tomography (PET), a nuclear medicine technique that detects and localizes radiation produced by positron-emitting radiopharmaceuticals administered exogenously to a subject [35]. Imaging glucose metabolism with ^{18}F -fluorodeoxyglucose (^{18}F -FDG) is most commonly used to provide functional information based on increased uptake and glycolysis of cancer cells [32,36]. ^{18}F -FDG PET is widely used in cancer diagnosis and screening, yet it is unsuitable for tumors in organs with high ^{18}F -FDG non-specific uptake such as the liver. Furthermore, it has limited ability to differentiate benign from metastatic lesions and early versus late stage disease [37].

The development of many other tracer types has given PET wide applications, particularly in the study of tumor metabolism [38]. Some preclinical PET tracers are probes consisting of a targeted molecule specific to a biological functional measurement attached to a radioisotope with a favorable half-life such as ^{11}C , ^{15}O and ^{18}F . Probes can also be used to image specific molecules based on binding of radiolabeled ligands (e.g., $\alpha 5\beta 3$ integrin imaging of tumor vasculature with radiolabeled glycosylated RGD (arginine-glycine-aspartate) containing peptides). A list of PET tracers used in preclinical studies and their biological targets is summarized in Table 2. PET has progressed to offer ~5 mm spatial resolution and picomolar sensitivity in clinical scanners [39]. Preclinical studies have

exploited microPET technology with comparable sensitivity and ~1 mm spatial resolution for treatment planning and response assessment [28,40].

Table 2. Summary of tracers used in preclinical studies and their biological targets.

Tracer	Targeting Moiety	Biological Target	Reference
⁶⁴ Cu	Anti-PD-1	Tumor infiltrating lymphocytes	[41]
¹²⁴ I	Anti-CD4	CD8+ cells	[42–44]
⁸⁹ Zr	Anti-CD4	T-cell reconstitution post-transplant	[43]
⁸⁹ Zr	Anti-CD3	tumor-infiltrating lymphocytes	[44]
⁶⁴ Cu	Anti-OX40	T cells activation	[45]
⁶⁸ Ga/ ¹⁸ F	Anti-CTLA-4	CTLA-4 visualization	[45]
¹⁸ F-FDG	PSMA	PSMA	[46]
¹⁸ F-FDG	Fluorodeoxyglucose	Glucose metabolism	[47]
⁶⁸ Ga-NODAGA-c(RGDfK)	RGD (arginine, glycine, aspartate) peptides	$\alpha\beta$ 3 integrins in the tumor vasculature	[48]
¹⁸ F-EF5	2-(2-Nitro-1H-imidazol-1-yl)-N-(2,2,3,3,3-pentafluoropropyl)-acetamide		[49,50]
¹⁸ F-FAZA	1-(5-fluoro-5-deoxy- α -D-arabinofuranosyl)-2-nitroimidazole	Hypoxia	
¹⁸ F-FMISO	Fluoromisonidazole		[51–54]
¹⁸ F-HX4	fluoro-2-(4-((2-nitro-1H-imidazol-1-yl)methyl)-1H-1,2,3-triazol-1-yl)propan-1-ol		
(¹⁸ F)F-AraG	2-(2-Nitro-1H-imidazol-1-yl)-N-(2,2,3,3,3-pentafluoropropyl)-acetamide fluoro-9- β -D-arabinofuranosyl guanine	T cell activation	[55,56]

Magnetic resonance imaging (MRI) has become an established medical imaging modality due to its superior soft tissue contrast and lack of ionizing radiation dose. MRI is based on combining high-strength magnetic fields with radiofrequency (RF) detection to exploit atomic nuclei with odd numbers of nucleons and thus net magnetic moments [28]. At the microscopic level, net magnetic fields in tissue depend on the microenvironment as well as the applied magnetic field, yielding soft tissue contrast uniquely characteristic of MRI. Preclinical MRI systems are being implemented for a range of applications, including MRI-guided radiation therapy for intracranial, pancreatic and flank tumors, immobilization devices, fiducial marker placement and MRI-only based treatment planning [57–59]. These methods are well established for mice and rats with technical developments towards implementing adaptable registration into existing workflows for small animal radiotherapy [57–59].

Other molecular imaging modalities such as BLI have been developed specifically for preclinical applications. BLI involves the engineering of cells to express a luciferase enzyme, which catalyzes the metabolism of a substrate (luciferin) that generates as a by-product a photon in the visible to near-infrared wavelength range [49]. Such enzymatic reactions are found natively in organisms including bacteria, fireflies, and jellyfish, however, molecular biology methods have allowed integration of luciferase into cells in vitro or into animals through the germline. Two-dimensional BLI is now used extensively in preclinical cancer biology research to detect, quantify, and localize specific cell types [60–62] and is being integrated with preclinical image-guided irradiators for target localization and response monitoring.

The X-Rad SmART (Precision X-ray, Inc, North Branford, CT, USA) offers a configuration in which a cooled CCD camera is mounted on the gantry perpendicular to the X-ray beam axis to allow two-dimensional BLI data to be collected from the subject and co-registered with the planning CT [15]. In contrast, the SARRP offers MuriGlo, an optical imaging system capable of both two-dimensional BLI, fluorescence imaging and three-dimensional bioluminescence tomography (BLT) [63]. Similarly, BLT has also been successfully integrated into the iSMAART system and shown accurately targeting with quantitative assessment of response in orthotopically implanted, luciferase expressing 4T1 breast cancer cells [64]. BLI is an attractive imaging modality in radiotherapy studies as it can provide target

localization information and does not contribute to added dose [65,66], however, research efforts are required to develop robust 3D reconstruction algorithms for true tomographical representation.

In addition to BLI, *in vivo* fluorescence imaging (FLI) is another optical imaging technique that is being applied to radiobiological studies. An interesting approach has been demonstrated combining the Cx225 platform with *intra-vital*, multimodal optical microscopy to study the spatio-temporal dynamics of tumor microvasculature in radiation response of tumors [67]. Another approach combined the iSMAART device with fluorescence molecular tomography (FMT) to localize tumors at depth with a localization error of <0.5 mm [19].

Finally, a number of imaging methods have been preclinically evaluated but have not been explored in the clinic. These include molecular ultrasound using microbubble agents, photoacoustic imaging, Raman spectroscopy, as well as a variety of emerging radiotracers, magnetic resonance imaging probes and X-ray contrast agents [28,34,46,68–70], which may yet provide important clinical advantages in diagnosis and treatment.

4. Translational Research Opportunities

Imaging techniques play a central role in patient management to determine tumor-specific characteristics and response to therapy. This is particularly evident in radiation oncology where imaging is used for diagnosis, treatment planning, response monitoring and to detect adverse effects resulting from treatment [35,71,72]. Preclinical investigations integrating anatomical, functional, and molecular imaging in the experimental study design allows interrogation of key molecular characteristics that can be used to detect and potentially predict radiotherapy response. CT and BLT have been successfully integrated with preclinical radiotherapy devices to provide excellent multi-modal imaging solutions. Using interchangeable beds and immobilization devices, it is also possible to develop sequential workflows across different systems allowing co-registration of multiple imaging sources with radiotherapy plans that are equally effective and more easily disseminated, e.g., sequential PET/MRI systems. Some of the unique research possibilities that these approaches are now enabling towards the realization of biologically optimized radiotherapy are explained below.

4.1. Quantifying Tumor Burden and Response to Therapy

Evaluation of the tumor burden at diagnosis and during response to therapy is critical in guiding treatment decisions, prognosis and radiotherapy planning. Clinically, longitudinal CT scans are used to assess volumetric differences in target lesions at baseline and after treatment, which are standardized to the Response Evaluation Criteria for Solid Tumors (RECIST) [73,74]. However, anatomical observations have limitations in imaging changes post treatment as they fail to accurately represent viable tumor cells. ¹⁸F-FDG-PET/CT has become established as an important tool in radiation oncology to determine primary tumor characteristics, lymph node invasion and metastases. This has led to the Positron Emission Tomography (PET) Response Criteria in Solid Tumors (PERCIST 1.0) which adopts functional imaging into routine assessment. These criteria also serve as a starting point for use in clinical trials when assessing the activity of novel therapies that stabilize disease, and has led to revised strategies based on functional rather than anatomical features [75].

Currently, no standardized staging or response criteria have been defined for preclinical studies where quantification of tumor burden is derived from caliper measurements or longitudinal monitoring of regions of interest delineated from imaging. In PET imaging, regions of interest are determined from the standardized uptake volume (SUV), defined as the level of tracer accumulation normalized to the subject mass. This may also be used to determine progression in cancer models by comparing tracer distributions in normal and diseased mice.

Preclinical efforts are needed towards optimizing PET tracers and evaluating radiotherapy response where determining success or failure may guide future treatment decisions such as dose boosting or salvage surgery. As tumor response is non-uniform, alterations in the SUVs of tracers often occurs prior to tissue changes and so may provide predictive information of response, local failure

or radioresistance. Preclinical evaluation of ^{18}F -FDG uptake has been determined for different doses and irradiated sub-volumes. This important study irradiated high uptake regions with high doses and reduced (redistribution approach) or standard doses (dose escalation approach) were delivered to the rest of the tumor volume. Minimum tumor growth delay was observed in the mice with dose escalation to the sub-volumes with high FDG uptake [47]. Other preclinical studies compare ^{18}F -FMISO, ^{18}F -FAZA and ^{18}F -HX4 to optimize imaging conditions to evaluate tumor hypoxia in preclinical models [52–54]. A further study used the hypoxia specific tracer ^{18}F -EF5 to determine changes in hypoxia with radiation response. Tracer uptake was correlated with tumor growth delay or total control and showed distinct responses corresponding to the uptake of ^{18}F -EF5 before irradiation, suggesting response can be predicted based on initial ^{18}F -EF5 uptake [49,50].

Finally, different imaging techniques can also allow differentiation of tumor and normal tissues at a level superior to anatomical imaging. Although technological improvements have reduced the risk of normal tissue injury, toxicity causing long-term side effects or interrupted treatment continues to occur in subsets of patients and can be critical in defining treatment options. Pre-clinically, CT data in free-breathing animals enabled the non-invasive and high-throughput detection of a range of pulmonary diseases in mice [76,77]. Moreover, CT was also used to image the radiation-induced lung fibrosis longitudinally for up to 9 months post irradiation [78–81]. MRI has also been used to detect pulmonary fibrosis in living mice and rats treated with bleomycin [82]. Considering the critical role of the immune system in radiotherapy response, imaging approaches capable of visualizing highly complex interactions involving multiple cell types are also being developed.

4.2. Imaging the Immune Response

The seminal discovery of enhanced antitumor immunity by blockade of the cytotoxic T-lymphocyte-associated protein 4 (CTLA-4) by Allison and colleagues in 1996 [83] has led to the rapid development and uptake of immunotherapy as standard of care for many types of cancer [84,85]. Currently, over 2000 different immunotherapy compounds are in development, with 26 approved immune-oncology (IO) agents already approved for use in the clinic including T-cell targeted immuno-modulators, cancer vaccines and cell therapies [85]. The underlying mechanism of action for IO agents often leads to abnormal response patterns termed pseudo-progression, and represents considerable risk in underestimating response which may lead to early removal of patients from treatment. This has resulted in the development of the iRECIST guidelines by the RECIST working group for the use of modified criteria in cancer immunotherapy trials [86], which provide information concerning tumor size but not biological characteristics of the tumor.

Given that only 15–30% of patients respond to IO agents as monotherapies, there is a critical need for biomarkers to accurately predict response and select patients most likely to respond, and for the development of novel combination therapies [87]. Radiotherapy is a promising approach for combination with IO due to its multiple immune-modulatory effects, which include natural killer (NK) cell activation [88], increased expression of tumor associated antigens [89] and activation of immunogenic cell death mediated by damage-associated molecular patterns (DAMPs) [87,90].

Limited information is available concerning the molecular imaging changes during response to IO agents as monotherapies or in combination with radiotherapy. Molecular imaging has much potential to differentiate immune response from tumor progression by targeted labelling of immune cells *ex vivo*, PET reporter gene expression or direct *in vivo* labelling and provides predictive biomarkers of response to IO in combination with radiotherapy [91]. Considering the observed dependence of immune effects on dose and fractionation scheme [92,93], major efforts are needed to optimize the combination of IO and radiotherapy in preclinical models prior to translation to the clinic. Important preclinical studies using syngeneic mouse mammary tumor models with small animal radiotherapy have delineated the mechanisms and dose response of radiation induced T cell activation through the DNA exonuclease, Trex1. These important findings may guide the selection of optimum radiation dose and fractionation in patients treated with immunotherapy [92]. Also, the tracer

2'-deoxy-2'-(¹⁸F)fluoro-9-β-D-arabinofuranosyl has been identified to have specific cytotoxicity in T-lymphocytes compared to other immune cell types and is currently under clinical investigation as an indicator of the immune status in cancer patients (NCT03142204). (¹⁸F)F-AraG has also been used in preclinical studies to image T-cell dynamics, showing up to 1.4-fold higher uptake in a Graft-versus-Host disease elicited by allogenic hematopoietic cell transplant compared to control mice [41,55,56].

4.3. Image-Guided Adaptive Radiotherapy

Anatomical changes during treatment including tumor growth, regression or weight loss may necessitate adaptive planning by modifying the treatment plan based on the most current image to prescribe new personalized margins and doses for individual patients [94]. Repeated CT imaging during treatment is often used for adaptive re-planning, aiming to integrate sequential imaging in the radiotherapy workflow. This has led to the development of MRI-integrated radiotherapy systems first conceptualized by Lagendijk and Bakker [95] with two systems now commercially available developed by ViewRay and the Philips Elekta Consortium [96,97].

In addition to real-time image-guided treatments, spatial variations in tracer uptake offer opportunities for dose boosting in sub-volumes of high ¹⁸F-FDG uptake or hypoxic regions [98–101]. Anatomical and functional imaging are proving essential in defining target volumes, in dose painting and adaptive treatments to optimize dose in radio-resistant areas, yet many challenges remain in how to best integrate these approaches and determine individualized treatments. Preclinical efforts have made towards developing novel technology, with several prototypes for MRI-PET imaging systems already developed and incorporated in pilot studies [101].

5. Conclusions

Technological innovations in the delivery of advanced conformal radiotherapy and radiological imaging have resulted in improved outcomes for cancer patients receiving radiotherapy. Clinical advances have been reverse translated to the laboratory, where research teams are now enabled to deliver highly conformal treatments to small volumes under image guidance. These advances fundamentally require a better understanding of the radiobiological correspondence between mice and humans so that fractionation schedules and dose distributions can be better interpolated in experimental models. The synergy of small animal radiotherapy studies with functional imaging has high potential to lead to the next generation of innovations in radiation oncology, which may include biologically guided treatments using predictive biomarkers to optimize dose, fractionation and combination treatments with IO or other molecular targeted agents.

Author Contributions: K.T.B., E.E.G., O.J.K., K.H.B. and M.G. conceptualized, wrote and reviewed the manuscript.

Funding: KHB is supported by a training Fellowship from the National Centre for the Replacement, Refinement and Reduction of Animals in Research (Grant Number NC/R001553/1). MG and KTB gratefully knowledge support from the Queen's Foundation, Queen's University Belfast.

Conflicts of Interest: The authors declare no conflict of interest.

References

1. Jaffray, D.A. Image-guided radiotherapy: From current concept to future perspectives. *Nat. Rev. Clin. Oncol.* **2012**, *9*, 688–699. [[CrossRef](#)] [[PubMed](#)]
2. Thariat, J.; Hannoun-Levi, J.-M.; Sun Myint, A.; Vuong, T.; Gérard, J.-P. Past, present, and future of radiotherapy for the benefit of patients. *Nat. Rev. Clin. Oncol.* **2012**, *10*, 52–60. [[CrossRef](#)] [[PubMed](#)]
3. Liu, F.-F.; Okunieff, P.; Bernhard, E.J.; Stone, H.B.; Yoo, S.; Coleman, C.N.; Vikram, B.; Brown, M.; Buatti, J.; Guha, C. Lessons Learned from Radiation Oncology Clinical Trials. *Clin. Cancer Res.* **2013**, *19*, 6089–6100. [[CrossRef](#)] [[PubMed](#)]

4. Bradley, J.D.; Paulus, R.; Komaki, R.; Masters, G.; Blumenschein, G.; Schild, S.; Bogart, J.; Hu, C.; Forster, K.; Magliocco, A.; et al. Standard-dose versus high-dose conformal radiotherapy with concurrent and consolidation carboplatin plus paclitaxel with or without cetuximab for patients with stage IIIA or IIIB non-small-cell lung cancer (RTOG 0617): A randomised, two-by-two factorial phase 3 study. *Lancet Oncol.* **2015**, *16*, 187–199. [[CrossRef](#)] [[PubMed](#)]
5. Hudson, A.A.; Chan, C.; Woolf, D.; Hiley, C.; Connor, J.O.; Bayman, N.; Blackhall, F.; Faivre-Finn, C.; Clara, C.; David, W. Is heterogeneity in stage 3 non-small cell lung cancer obscuring the potential benefits of dose-escalated concurrent chemo-radiotherapy in clinical trials? *Lung Cancer* **2018**, *118*, 139–147. [[CrossRef](#)] [[PubMed](#)]
6. Stone, H.B.; Bernhard, E.J.; Coleman, C.N.; Deye, J.; Capala, J.; Mitchell, J.B.; Brown, J.M. Preclinical Data on Efficacy of 10 Drug-Radiation Combinations: Evaluations, Concerns, and Recommendations. *Transl. Oncol.* **2016**, *9*, 46–56. [[CrossRef](#)] [[PubMed](#)]
7. Coleman, C.N.; Higgins, G.S.; Brown, J.M.; Baumann, M.; Kirsch, D.G.; Willers, H.; Prasanna, P.G.S.; Dewhurst, M.W.; Bernhard, E.J.; Ahmed, M.M. Improving the predictive value of preclinical studies in support of radiotherapy clinical trials. *Clin. Cancer Res.* **2016**, *22*, 3138–3147. [[CrossRef](#)]
8. Dilworth, J.T.; Krueger, S.A.; Wilson, G.D.; Marples, B. Preclinical Models for Translational Research Should Maintain Pace With Modern Clinical Practice. *Radiat. Oncol. Biol.* **2013**, *88*, 540–544. [[CrossRef](#)]
9. Regaud, C.; Nogier, T. Stérilisation reontgénienne, totale et définitive, sans radiodermite, des testicules du belier adulte. *C. R. Soc. Biol.* **1911**, *70*, 202–203.
10. Perlman, R.L. Mouse models of human disease: An evolutionary perspective. *Evol. Med. Public Health* **2016**, *2016*, 170–176. [[CrossRef](#)]
11. Fox, J.G.; Barthold, S.W.; Davisson, M.T.; Newcomer, C.E.; Quimby, F.W.; Smith, A.L. *The Mouse in Biomedical Research*, 2nd ed.; Elsevier Inc.: Oxford, UK, 2007; ISBN 9780123694546.
12. Tratar, U.L.; Horvat, S.; Cemazar, M. Transgenic Mouse Models in Cancer Research. *Front. Oncol.* **2018**, *8*, 268. [[CrossRef](#)]
13. Koontz, B.F.; Verhaegen, F.; De Ruyscher, D. Tumour and normal tissue radiobiology in mouse models: How close are mice to mini-humans? *Br. J. Radiol.* **2016**, *90*, 20160441. [[CrossRef](#)]
14. Wong, J.; Armour, E.; Kazanzides, P.; Iordachita, I.; Tryggstad, E.; Deng, H.; Matinfar, M.; Kennedy, C.; Liu, Z.; Chan, T.; et al. High-Resolution, Small Animal Radiation Research Platform With X-Ray Tomographic Guidance Capabilities. *Int. J. Radiat. Oncol. Biol. Phys.* **2008**, *71*, 1591–1599. [[CrossRef](#)] [[PubMed](#)]
15. Cho, N.; Tsiamas, P.; Velarde, E.; Tryggstad, E.; Jacques, R.; Berbeco, R.; McNutt, T.; Kazanzides, P.; Wong, J. Validation of GPU-accelerated superposition—Convolution dose computations for the Small Animal Radiation Research Platform. *Med. Phys.* **2018**, *45*, 2252–2265. [[CrossRef](#)] [[PubMed](#)]
16. Weersink, R.A.; Ansell, S.; Wang, A.; Wilson, G.; Shah, D.; Lindsay, P.E.; Jaffray, D.A. Integration of optical imaging with a small animal irradiator. *Med. Phys.* **2018**, *45*, 102701. [[CrossRef](#)] [[PubMed](#)]
17. Sha, H.; Udayakumar, T.S.; Johnson, P.B.; Dogan, N.; Pollack, A.; Yang, Y. An image guided small animal stereotactic radiotherapy system. *Oncotarget* **2016**, *7*, 18825. [[CrossRef](#)]
18. Shi, J.; Udayakumar, T.S.; Wang, Z.; Dogan, N.; Pollack, A.; Yang, Y. Optical molecular imaging-guided radiation therapy part 1: Integrated x-ray and bioluminescence tomography. *Med. Phys.* **2018**, *44*, 4786–4794. [[CrossRef](#)]
19. Shi, J.; Udayakumar, T.S.; Wang, Z.; Dogan, N.; Pollack, A. Optical molecular imaging-guided radiation therapy part 2: Integrated x-ray and fluorescence molecular tomography. *Med. Phys.* **2018**, *45*, 2252–2265. [[CrossRef](#)]
20. Tillner, F.; Thute, P.; Löck, S.; Dietrich, A.; Fursov, A.; Haase, R.; Lukas, M.; Rimarzig, B.; Sobiella, M.; Krause, M.; et al. Precise image-guided irradiation of small animals: A flexible non-profit platform. *Phys. Med. Biol.* **2016**, *61*, 3084–3108. [[CrossRef](#)]
21. Sharma, S.; Narayanasamy, G.; Przybyla, B.; Webber, J.; Boerma, M.; Clarkson, R.; Moros, E.G.; Corry, P.M.; Griffin, R.J. Advanced Small Animal Conformal Radiation Therapy Device. *Technol. Cancer Res. Treat.* **2016**, *16*, 45–56. [[CrossRef](#)]
22. Hou, Z.; Rodriguez, M.; van den Fred, H.; Nelson, G.; Jogani, R.; Xu, J.; Zhu, X.; Xian, Y.; Tran, P.; Welsher, D.W.; et al. Development of a micro-computed tomography—Bades image-guided conformal radiotherapy system for small animals. *Int. J. Radiat. Oncol. Biol. Phys.* **2010**, *78*, 297–305. [[CrossRef](#)]

23. Felix, M.C.; Fleckenstein, J.; Kirschner, S.; Hartmann, L.; Wenz, F.; Brockmann, M.A.; Glatting, G.; Giordano, F.A. Image-guided radiotherapy using a modified industrial micro-CT for preclinical applications. *PLoS ONE* **2015**, *10*, e0126246. [[CrossRef](#)] [[PubMed](#)]
24. Jensen, M.D.; Holdsworth, D.W.; Drangova, M. Implementation and commissioning of an integrated micro-CT/RT system with computerized independent jaw collimation. *Med. Phys.* **2013**, *40*, 081706. [[CrossRef](#)] [[PubMed](#)]
25. Jacques, R.; Wong, J.; Taylor, R.; McNutt, T. Real-time dose computation: GPU-accelerated source modeling and superposition/convolution. *Med. Phys.* **2011**, *38*, 294–305. [[CrossRef](#)] [[PubMed](#)]
26. Verhaegen, F.; van Hoof, S.; Granton, P.V.; Trani, D. A review of treatment planning for precision image-guided photon beam pre-clinical animal radiation studies. *Z. Med. Phys.* **2014**, *24*, 323–334. [[CrossRef](#)] [[PubMed](#)]
27. Verhaegen, F.; Dubois, L.; Gianolini, S.; Hill, M.A.; Karger, C.P.; Lauber, K.; Prise, K.M.; Sarrut, D.; Thorwarth, D.; Vanhove, C.; et al. ESTRO ACROP Guideline ESTRO ACROP: Technology for precision small animal radiotherapy research: Optimal use and challenges. *Radiother. Oncol.* **2018**, *126*, 471–478. [[CrossRef](#)] [[PubMed](#)]
28. Kiessling, F. *Small Animal Imaging Basics and Practical Guide*, 2nd ed.; Kiessling, F., Pichler, B.J., Hauff, P., Eds.; Springer International Publishing AG: New York, NY, USA, 2011; ISBN 9783319422008.
29. Prescott, M.J.; Lidster, K. Perspective Focus on Reproducibility Improving quality of science through better animal welfare: The NC3Rs strategy Focus on Reproducibility Perspective. *Nat. Publ. Gr.* **2017**, *46*, 152–156. [[CrossRef](#)]
30. Vaidya, T.; Agrawal, A.; Mahajan, S.; Thakur, M.H.; Mahajan, A. The Continuing Evolution of Molecular Functional Imaging in Clinical Oncology: The Road to Precision Medicine and Radiogenomics (Part I). *Mol. Diagn. Ther.* **2018**. [[CrossRef](#)]
31. Mankoff, D. A Definition of Molecular Imaging. *J. Nucl. Med.* **2007**, *48*, 21–23.
32. Ben-Haim, S.; Ell, P. PET and PET/CT in the Evaluation of Cancer Treatment Response. *J. Nucl. Med.* **2009**, *50*, 88–99. [[CrossRef](#)]
33. Plathow, C.; Weber, W.A. Tumor Cell Metabolism Imaging. *J. Nucl. Med.* **2008**, *49*, 43S–63S. [[CrossRef](#)] [[PubMed](#)]
34. Gambhir, S.S.; Yaghoubi, S.S. *Molecular Imaging with Reporter Genes*; Cambridge University Press: Cambridge, MA, USA, 2010; ISBN 9780511730405.
35. Gambhir, S.S. Molecular imaging of cancer with positron emission tomography. *Nat. Rev. Cancer* **2002**, *2*, 683–693. [[CrossRef](#)] [[PubMed](#)]
36. Fletcher, J.W.; Djulbegovic, B.; Soares, H.P.; Siegel, B.A.; Lowe, V.J.; Lyman, G.H.; Coleman, R.E.; Wahl, R.; Paschold, J.C.; Avril, N.; et al. Recommendations on the Use of PET in Oncology. *J. Nucl. Med.* **2018**, *49*, 480–509. [[CrossRef](#)] [[PubMed](#)]
37. Tichauer, K.M.; Wang, Y.; Pogue, B.W.; Liu, J.T.C. Quantitative in vivo cell-surface receptor imaging in oncology: Kinetic modeling & paired-agent principles from nuclear medicine and optical imaging. *Phys. Med. Biol.* **2016**, *60*, R239. [[CrossRef](#)]
38. Ntziachristos, V.; Pleitez, M.A.; Aime, S.; Brindle, K.M. Emerging Technologies to Image Tissue Metabolism. *Cell Metab.* **2019**. [[CrossRef](#)] [[PubMed](#)]
39. Watanabe, M.; Saito, A.; Isobe, T.; Ote, K. Performance evaluation of a high-resolution brain PET scanner using four-layer MPPC DOI Performance evaluation of a high-resolution brain PET scanner using four-layer MPPC DOI detectors. *Phys. Med. Biol.* **2017**, *62*, 7148. [[CrossRef](#)]
40. Raylman, R.R.; Stolin, A.V.; Martone, P.F.; Smith, M.F. TandemPET—A High Resolution, Small Animal, Virtual Pinhole-Based PET Scanner: Initial Design Study. *IEEE Trans. Nucl. Sci.* **2017**, *63*, 75–83. [[CrossRef](#)]
41. Natarajan, A.; Mayer, A.T.; Reeves, R.E.; Nagamine, C.M.; Gambhir, S.S. Development of Novel ImmunoPET Tracers to Image Human PD-1 Checkpoint Expression on Tumor-Infiltrating Lymphocytes in a Humanized Mouse Model. *Mol. Imaging Biol.* **2017**, *19*, 903–914. [[CrossRef](#)]
42. Knowles, S.M.; Wu, A.M. Advances in Immuno-Positron Emission Tomography: Antibodies for Molecular Imaging in Oncology. *J. Clin. Oncol.* **2012**, *30*, 3884. [[CrossRef](#)]
43. Tavaré, R.; Escuin-Ordinas, H.; Mok, S.; Mccracken, M.N.; Kirstin, A.; Tavaré, R. An Effective Immuno-PET Imaging Method to Monitor CD8-Dependent Responses to Immunotherapy. *Cancer Res.* **2016**. [[CrossRef](#)]

44. Vera, D.R.B.; Smith, C.C.; Bixby, L.M.; Glatt, D.M.; Dunn, S.; Saito, R.; Kim, W.Y.; Serody, J.S.; Vincent, G.; Parrott, M.C. Immuno-PET imaging of tumor-infiltrating lymphocytes using zirconium-89 radiolabeled anti-CD3 antibody in immune-competent mice bearing syngeneic tumors. *PLoS ONE* **2018**, *13*, e0193832.
45. Alam, I.S.; Mayer, A.T.; Sagiv-Barfi, I.; Wang, K.; Vermesh, O.; Czerwinski, D.K.; Johnson, E.M.; James, M.L.; Levy, R.; Gambhir, S.S. Imaging activated T cells predicts response to cancer vaccines. *J. Clin. Investig.* **2018**, *128*, 2569–2580. [[CrossRef](#)] [[PubMed](#)]
46. Kuo, H.; Merkens, H.; Zhang, Z.; Uribe, C.F.; Zhang, C.; Colpo, N.; Lin, K.; Benard, F. Enhancing treatment efficacy of ¹⁷⁷Lu-PSMA-617 with the conjugation of an albumin-binding motif: Preclinical dosimetry and endoradiotherapy studies. *Mol. Pharm.* **2018**, *15*, 5183–5191. [[CrossRef](#)] [[PubMed](#)]
47. Trani, D.; Yaromina, A.; Dubois, L.; Granzier, M.; Peeters, S.G.J.A.; Biemans, R.; Nalbantov, G.; Lieuwes, N.; Reniers, B.; Troost, E.E.G.C.; et al. Preclinical Assessment of Efficacy of Radiation Dose Painting Based on Intratumoral FDG-PET Uptake. *Clin. Cancer Res.* **2015**, *21*, 5511–5519. [[CrossRef](#)] [[PubMed](#)]
48. Rylova, S.N.; Barnucz, E.; Fani, M.; Braun, F.; Werner, M.; Lassmann, S.; Maecke, H.R.; Weber, W.A. Does Imaging avb3 Integrin Expression with PET Detect Changes in Angiogenesis During Bevacizumab Therapy? *J. Nucl. Med.* **2018**, *55*, 1878–1884. [[CrossRef](#)] [[PubMed](#)]
49. Koch, C.J.; Shuman, A.L.; Jenkins, W.T.; Kachur, A.V.; Karp, J.S.; Freifelder, R.; Dolbier, W.R., Jr.; Evans, S.M. The radiation response of cells from 9L gliosarcoma tumours is correlated with [F18]-EF5 uptake. *Int. J. Radiat. Biol.* **2009**, *85*, 1137–1147. [[CrossRef](#)]
50. Ali, R.; Apte, S.; Vilalta, M.; Subbarayan, M.; Miao, Z.; Chin, F.T.; Graves, E.E. ¹⁸F-EF5 PET is predictive of response to fractionated radiotherapy in preclinical tumor models. *PLoS ONE* **2015**, *10*, e0139425. [[CrossRef](#)] [[PubMed](#)]
51. Grkovski, M.; Fanchon, L.; Vara, N.; Pillarsetty, K.; Russell, J.; Humm, J.L. F-fluoromisonidazole predicts evofosfamide uptake in pancreatic tumor model. *EJNMMI Res.* **2018**, *8*, 53. [[CrossRef](#)]
52. Jans, H.; Yang, X.; Brocks, D.R.; Kumar, P.; Wuest, M.; Wiebe, L.I. Positron Emission Tomography (PET) and Pharmacokinetics: Classical Blood Sampling Versus Image-Derived Analysis of [18 F] FAZA and [18 F] FDG in a Murine Tumor Bearing Model. *J. Pharm. Pharm. Sci.* **2018**, *21*, 32s–47s.
53. Dubois, L.J.; Lieuwes, N.G.; Janssen, M.H.M.; Peeters, W.J.M.; Windhorst, A.D. Preclinical evaluation and validation of [18F]HX4, a promising hypoxia marker for PET imaging. *Proc. Natl. Acad. Sci. USA* **2011**. [[CrossRef](#)]
54. Peeters, S.G.J.A.; Zegers, C.M.L.; Lieuwes, N.G.; Van Elmpt, W.; Eriksson, J.; Van Dongen, G.A.M.S.; Dubois, L.; Lambin, P. A Comparative Study of the Hypoxia PET Tracers [18 F] HX4, [18 F] FAZA, and [18 F] FMISO in a Preclinical Tumor Model. *Radiat. Oncol. Biol.* **2015**, *91*, 351–359. [[CrossRef](#)] [[PubMed](#)]
55. Ronald, J.A.; Kim, B.-S.; Gowrishankar, G.; Namavari, M.; Alam, I.S.; D'Souza, A.; Nishikii, H.; Chuang, H.-Y.; Ilovich, O.; Lin, C.-F.; et al. A PET Imaging Strategy to Visualize Activated T Cells in Acute Graft-versus-Host Disease Elicited by Allogeneic Hematopoietic Cell Transplant. *Cancer Res.* **2017**, *77*, 2893–2902. [[CrossRef](#)] [[PubMed](#)]
56. Namavari, M.; Chang, Y.F.; Kusler, B.; Yaghoubi, S.; Mitchell, B.S.; Gambhir, S.S. Synthesis of 2'-Deoxy-2'-[18F]fluoro-9-β-DArabinofuranosylguanine: A novel agent for imaging T-cell activation with PET. *Mol. Imaging Biol.* **2011**, *13*, 812–818. [[CrossRef](#)] [[PubMed](#)]
57. Dobiasch, S.; Kampfer, S.; Habermehl, D.; Duma, M.N.; Felix, K.; Strauss, A.; Schilling, D.; Wilkens, J.J.; Combs, S.E. MRI-based high-precision irradiation in an orthotopic pancreatic tumor mouse model. *Strahlentherapie und Onkologie* **2018**, *194*, 944–952. [[CrossRef](#)]
58. Bolcaen, J.; Descamps, B.; Deblaere, K.; Boterberg, T.; Hallaert, G.; Van den Broecke, C.; Decrock, E.; Vral, A.; Leybaert, L.; Vanhove, C.; et al. MRI-guided 3D conformal arc micro-irradiation of a F98 glioblastoma rat model using the Small Animal Radiation Research Platform (SARRP). *J. Neuro-Oncol.* **2014**, *120*, 257–266. [[CrossRef](#)] [[PubMed](#)]
59. Black, P.J.; Smith, D.R.; Chaudhary, K.; Xanthopoulos, E.P.; Chin, C.; Spina, C.S.; Hwang, M.E.; Mayeda, M.; Wang, Y.; Connolly, E.P.; et al. Velocity-based Adaptive Registration and Fusion for Fractionated Stereotactic Radiosurgery Using the Small Animal Radiation Research Platform. *Radiat. Oncol. Biol.* **2018**, *15*, 841–847. [[CrossRef](#)] [[PubMed](#)]

60. Rafat, M.; Aguilera, T.A.; Vilalta, M.; Bronsart, L.L.; Soto, L.A.; von Eyben, R.; Golla, M.A.; Ahrari, Y.; Melemenidis, S.; Afghahi, A.; et al. Macrophages Promote Circulating Tumor Cell-Mediated Local Recurrence Following Radiation Therapy in Immunosuppressed Patients. *Cancer Res.* **2018**, *78*, 4241–4253. [[CrossRef](#)] [[PubMed](#)]
61. Vilalta, M.; Brune, J.; Rafat, M.; Soto, L.; Graves, E.E. The role of granulocyte macrophage colony stimulating factor (GM-CSF) in radiation-induced tumor cell migration. *Clin. Exp. Metastasis* **2018**, *35*, 247–254. [[CrossRef](#)]
62. Jones, L.; Richmond, J.; Evans, K.; Carol, H.; Jing, D.; Kurmasheva, R.T.; Billups, C.A.; Houghton, P.J.; Smith, M.A.; Lock, R.B. Bioluminescence Imaging Enhances Analysis of Drug Responses in a Patient-Derived Xenograft Model of Pediatric ALL. *Clin. Cancer Res.* **2017**, *23*, 3744–3755. [[CrossRef](#)]
63. Zhang, B.; Wang, K.K.H.; Yu, J.; Eslami, S.; Iordachita, I.; Reyes, J.; Malek, R.; Tran, P.T.; Patterson, M.S.; Wong, J.W. Bioluminescence Tomography-Guided Radiation Therapy for Preclinical Research. *Int. J. Radiat. Oncol. Biol. Phys.* **2016**, *94*, 1144–1153. [[CrossRef](#)]
64. Shi, J.; Udayakumar, T.S.; Xu, K.; Dogan, N.; Pollack, A.; Yang, Y. Bioluminescence Tomography Guided Small-Animal Radiation Therapy and Tumor Response Assessment. *Radiat. Oncol. Biol.* **2018**, *102*, 848–857. [[CrossRef](#)] [[PubMed](#)]
65. Iglesias, V.S.; Van Hoof, S.J.; Vaniqui, A.; Schyns, L.E.J.R. Small animal IGRT special feature: Full Paper An orthotopic non-small cell lung cancer model for image-guided small animal radiotherapy platforms. *Br. J. Radiol.* **2019**, *91*, 20180476.
66. Fricke, I.B.; De Souza, R.; Costa Ayub, L.; Francia, G.; Kerbel, R.; Jaffray, D.A.; Zheng, J. Spatiotemporal assessment of spontaneous metastasis formation using multimodal in vivo imaging in HER2+ and triple negative metastatic breast cancer xenograft models in mice. *PLoS ONE* **2018**, *13*, e0196892. [[CrossRef](#)] [[PubMed](#)]
67. Maeda, A.; Leung, M.K.K.; Conroy, L.; Chen, Y.; Bu, J.; Lindsay, P.E.; Mintzberg, S.; Virtanen, C.; Tsao, J.; Winegarden, N.A.; et al. In Vivo Optical Imaging of Tumor and Microvascular Response to Ionizing Radiation. *PLoS ONE* **2012**, *7*, e42133. [[CrossRef](#)]
68. Davis, R.M.; Kiss, B.; Trivedi, D.R.; Metzner, T.J.; Liao, J.C.; Gambhir, S.S. Surface-Enhanced Raman Scattering Nanoparticles for Multiplexed Imaging of Bladder Cancer Tissue Permeability and Molecular Phenotype. *ACS Nano* **2018**, *12*, 9669–9679. [[CrossRef](#)]
69. Kiess, A.P.; Banerjee, S.R.; Mease, R.C.; Rowe, S.P.; Rao, A.; Foss, C.A.; Yang, X.; Cho, S.Y.; Nimmagadda, S.; Pomper, M.G.; et al. Prostate-specific membrane antigen as a target for cancer imaging and therapy. *Q. J. Nucl. Med. Mol. Imaging* **2015**, *59*, 241–268.
70. Tse, B.W.; Cowin, G.J.; Soekmadji, C.; Jovanovic, L.; Vasireddy, R.S.; Ling, M.T.; Khatri, A.; Liu, T.; Thierry, B.; Russell, P.J. PSMA-targeting iron oxide magnetic nanoparticles enhance MRI of preclinical prostate cancer. *Nanomedicine* **2015**, *10*, 375–386. [[CrossRef](#)] [[PubMed](#)]
71. Smith-bindman, R.; Miglioretti, D.L.; Larson, E.B. Rising Use Of Diagnostic Medical Imaging In A Large Integrated Health System. *Health Aff.* **2008**, *27*, 1491–1502. [[CrossRef](#)]
72. Rowlands, J.A. Diagnostic imaging over the last 50 years: Research and development in medical imaging science and technology. *Phys. Med. Biol.* **2006**, *51*, R5. [[CrossRef](#)]
73. Therasse, P.; Arbuck, S.G.; Eisenhauer, E.A.; Wanders, J.; Kaplan, R.S.; Rubinstein, L.; Verweij, J.; Van Glabbeke, M.; van Oosterom, A.T.; Christian, M.C.; et al. New guidelines to evaluate the response to treatment in solid tumors. European Organization for Research and Treatment of Cancer, National Cancer Institute of the United States, National Cancer Institute of Canada. *J. Natl. Cancer Inst.* **2000**, *92*, 205–216. [[CrossRef](#)]
74. Schwartz, L.H.; Litière, S.; de Vries, E.; Ford, R.; Gwyther, S.; Mandrekar, S.; Shankar, L.; Bogaerts, J.; Chen, A.; Dancey, J.; et al. RECIST 1.1—Update and clarification: From the RECIST committee. *Eur. J. Cancer* **2016**, *62*, 132–137. [[CrossRef](#)] [[PubMed](#)]
75. Wahl, R.L.; Jacene, H.; Kasamon, Y.; Lodge, M.A. From RECIST to PERCIST: Evolving Considerations for PET Response Criteria in Solid Tumors. *J. Nucl. Med.* **2009**, *50* (Suppl. 1), 122S–150S. [[CrossRef](#)]
76. Gammon, S.T.; Foje, N.; Brewer, E.M.; Owers, E.; Downs, C.A.; Budde, M.D.; Leevy, W.M.; Helms, M.N. Real-time Visualization of Lung Function: From Micro to Macro Preclinical anatomical, molecular, and functional imaging of the lung with multiple modalities. *Am. J. Physiol.-Lung Cell. Mol. Physiol.* **2014**, *306*, L897–L914. [[CrossRef](#)] [[PubMed](#)]

77. Ghita, M.; Dunne, V.; Hanna, G.G.; Prise, K.M.; Williams, J.P.; Butterworth, K.T. Preclinical models of radiation induced lung damage: Challenges and opportunities for small animal radiotherapy. *Br. J. Radiol.* **2019**, *92*, 20180473. [[CrossRef](#)] [[PubMed](#)]
78. Granton, P.V.; Dubois, L.; Van Elmpt, W.; Van Hoof, S.J.; Lieuwes, N.G.; De Ruyscher, D.; Verhaegen, F. A longitudinal evaluation of partial lung irradiation in mice by using a dedicated image-guided small animal irradiator. *Int. J. Radiat. Oncol. Biol. Phys.* **2014**, *90*, 696–704. [[CrossRef](#)]
79. De Ruyscher, D.; Granton, P.V.; Lieuwes, N.G.; van Hoof, S.; Wollin, L.; Weynand, B.; Dingemans, A.M.; Verhaegen, F.; Dubois, L. Nintedanib reduces radiation-induced microscopic lung fibrosis but this cannot be monitored by CT imaging: A preclinical study with a high precision image-guided irradiator. *Radiother. Oncol.* **2017**, *124*, 482–487. [[CrossRef](#)] [[PubMed](#)]
80. Dunne, V.; Ghita, M.; Small, D.M.; Coffey, C.B.M.; Weldon, S.; Taggart, C.C.; Osman, S.O.; McGarry, C.K.; Prise, K.M.; Hanna, G.G.; et al. Inhibition of ataxia telangiectasia related-3 (ATR) improves therapeutic index in preclinical models of non-small cell lung cancer (NSCLC) radiotherapy. *Radiother. Oncol.* **2017**, *124*, 475–481. [[CrossRef](#)]
81. Ghita, M.; Dunne, V.; McMahon, S.J.; Osman, S.O.; Small, D.M.; Weldon, S.; Taggart, C.C.; McGarry, C.K.; Hounsell, A.R.; Graves, E.E.; et al. Preclinical Evaluation of Dose-Volume Effects and Lung Toxicity Occurring in- and out-of-field. *Int. J. Radiat. Oncol. Biol. Phys.* **2018**. [[CrossRef](#)]
82. Egger, C.; Gérard, C.; Vidotto, N.; Accart, N.; Cannet, C.; Dunbar, A.; Tigani, B.; Piaia, A.; Jarai, G.; Jarman, E.; et al. Lung volume quantified by MRI reflects extracellular-matrix deposition and altered pulmonary function in bleomycin models of fibrosis: Effects of SOM230. *Am. J. Physiol.-Lung Cell. Mol. Physiol.* **2018**, *306*, L1064–L1077. [[CrossRef](#)]
83. Leach, D.R.; Krummel, M.F.; Allison, J.P. Enhancement of antitumor immunity by CTLA-4 blockade. *Science* **1996**, *271*, 1734–1736. [[CrossRef](#)]
84. Couzin-Frankel, J. Cancer Immunotherapy. *Science (80-)* **2013**, *342*, 1432–1433. [[CrossRef](#)] [[PubMed](#)]
85. Tang, J.; Shalabi, A.; Hubbard-Lucey, V.M. Comprehensive analysis of the clinical immuno-oncology landscape. *Ann. Oncol.* **2018**, *29*, 84–91. [[CrossRef](#)] [[PubMed](#)]
86. Seymour, L.; Bogaerts, J.; Perrone, A.; Ford, R.; Schwartz, L.H.; Mandrekar, S.; Lin, N.U.; Litière, S.; Dancey, J.; Chen, A.; et al. iRECIST: Guidelines for response criteria for use in trials testing immunotherapeutics. *Lancet Oncol.* **2017**, *18*, e143–e152. [[CrossRef](#)]
87. Lhuillier, C.; Vanpouille-Box, C.; Galluzzi, L.; Chiara, S. Emerging biomarkers for the combination of radiotherapy and immune checkpoint blockers. *Semin. Cancer Biol.* **2018**, *52*, 125–134. [[CrossRef](#)] [[PubMed](#)]
88. Gonzalez, S.; Smyth, M.J.; Galluzzi, L.; Lo, A. Control of Metastasis by NK Cells. *Cancer Cell* **2017**, *32*, 135–154. [[CrossRef](#)]
89. Garnett, C.T.; Palena, C.; Chakarborty, M.; Tsang, K.; Schlom, J.; Hodge, J.W. Sublethal Irradiation of Human Tumor Cells Modulates Phenotype Resulting in Enhanced Killing by Cytotoxic T Lymphocytes. *Cancer Res.* **2004**, *64*, 7985–7994. [[CrossRef](#)] [[PubMed](#)]
90. Galluzzi, L.; Buqué, A.; Kepp, O.; Zitvogel, L.; Kroemer, G. Immunogenic cell death in cancer and infectious disease. *Nat. Publ. Gr.* **2016**, *17*, 97–111. [[CrossRef](#)]
91. Van Der Veen, E.L.; Bensch, F.; Glaudemans, A.W.J.M.; Hooge, M.N.L.; Vries, E.G.E. De Molecular imaging to enlighten cancer immunotherapies and underlying involved processes. *Cancer Treat. Rev.* **2018**, *70*, 232–244. [[CrossRef](#)]
92. Vanpouille-Box, C.; Alard, A.; Aryankalayil, M.J.; Sarfraz, Y.; Diamond, J.M.; Schneider, R.J.; Inghirami, G.; Coleman, C.N.; Formenti, S.C.; Demaria, S. DNA exonuclease Trex1 regulates radiotherapy-induced tumour immunogenicity. *Nat. Commun.* **2017**, *8*, 15618. [[CrossRef](#)]
93. Vanpouille-box, C.; Formenti, S.C.; Demaria, S. TREX1 dictates the immune fate of irradiated cancer cells. *Oncoimmunology* **2017**, *6*, e1339857. [[CrossRef](#)]
94. Yan, D. Adaptive Radiotherapy: Merging Principle Into Clinical Practice. *Semin. Radiat. Oncol.* **2010**, *20*, 79–83. [[CrossRef](#)]
95. Lagendijk, J.J.W.; Van Vulpen, M.; Raaymakers, B.W. The development of the MRI linac system for online MRI-guided radiotherapy: A clinical update. *J. Intern. Med.* **2016**, *280*, 203–208. [[CrossRef](#)] [[PubMed](#)]

96. Mutic, S.; Low, D.; Chmielewski, T.; Fought, G.; Gerganov, G.; Hernandez, M.; Kawrakow, I.; Kishawi, E.; Kuduvalli, G.; Sharma, A.; et al. The Design and Implementation of a Novel Compact Linear Accelerator-Based Magnetic Resonance Imaging-Guided Radiation Therapy (MR-IGRT) System. *Radiat. Oncol. Biol.* **2016**, *96*, E641. [[CrossRef](#)]
97. Raaijmakers, A.; Raaymakers, B.; van der Meer, S.; Lagendijk, J.J.W. Integrating a MRI scanner with a 6 MV radiotherapy accelerator: Impact of the surface orientation on the entrance and exit dose due to the transverse magnetic field Integrating a MRI scanner with a 6 MV radiotherapy accelerator: Impact of the surface or. *Phys. Med. Biol.* **2007**, *52*, 929–939. [[CrossRef](#)] [[PubMed](#)]
98. Hanna, G.G.; Koste, D.; Dahele, M.R.; Carson, K.J.; Haasbeek, C.J.A.; Migchielsen, R.; Hounsell, A.R.; Senan, S. Defining Target Volumes for Stereotactic Ablative Radiotherapy of Early-stage Lung Tumours: A Comparison of Three-dimensional 18 F-fluorodeoxyglucose Positron Emission Tomography and Four-dimensional Computed Tomography q. *Clin. Oncol.* **2012**, *24*, e71–e80. [[CrossRef](#)] [[PubMed](#)]
99. Aerts, H.J.W.L.; Lambin, P.; Ruyscher, D. De FDG for dose painting: A rational choice. *Radiother. Oncol.* **2010**, *97*, 163–164. [[CrossRef](#)] [[PubMed](#)]
100. Choi, W.; Lee, S.; Ho, S.; Sook, J.; Joon, S.; Chun, K.; Kyung, E.; Hoon, J.; Hoon, S.; Kim, S.; et al. Planning study for available dose of hypoxic tumor volume using fluorine-18-labeled fluoromisonidazole positron emission tomography for treatment of the head and neck cancer. *Radiother. Oncol.* **2010**, *97*, 176–182. [[CrossRef](#)] [[PubMed](#)]
101. Judenhofer, M.S.; Cherry, S.R. Applications for Preclinical PET/MRI. *Semin. Nucl. Med.* **2013**, *43*, 19–29. [[CrossRef](#)]



© 2019 by the authors. Licensee MDPI, Basel, Switzerland. This article is an open access article distributed under the terms and conditions of the Creative Commons Attribution (CC BY) license (<http://creativecommons.org/licenses/by/4.0/>).